Physicochem. Probl. Miner. Process., 54(3), 2018, 965-974

http://www.journalssystem.com/ppmp

Physicochemical Problems of Mineral Processing

ISSN 1643-1049

Received January 10, 2018; accepted March 20, 2018

Kinetic research of quinoline, pyridine and phenol adsorption on modified coking coal

Xianfeng Sun [1], Hongxiang Xu [1], Junfeng Wang [2], Kejia Ning [1], Gen Huang [1], Yuexian Yu [1], Liqiang Ma [1]

[1] School of Chemical Engineering and Technology, China University of Mining & Technology (Beijing) Beijing 100083, China

[2] National Key Laboratory of Biochemical Engineering, Institute of Process Engineering, Chinese Academy of Sciences Beijing 100190, China

Corresponding author: xuhongxiang001@163.com (H.X. Xu); huanggencumt@163.com (G. Huang)

Abstract: Adsorption is widely used in wastewater treatment. In this work, the removal of quinoline, pyridine and phenol from coking wastewater by using modified coking coal, which was treated by four different modification methods i.e. acidification sodium hydroxide (5 mol/dm3), hydrochloric acid (5 mol/dm3) and acetic acid (5 mol/dm3) and low-temperature (105℃) oxidation, was investigated. The modified coal was characterized by the surface area analysis, SEM, total acidity and basicity and FT-IR. The results showed that the surface area from high to low follows the order: modification with acetic acid, modification with hydrochloric acid, raw coal, modification with sodium hydroxide and modification with low-temperature. Experimental data were fitted to pseudo-first-order, pseudo-second-order and intra-particle diffusion. The adsorption of all followed pseudo-second-order kinetics. The result showed that the removal efficiency of coal modified by hydrochloric acid and acetic acid are higher than raw coal, while modified by sodium hydroxide and low-temperature are lower than raw coal., The coal modified by hydroxide acid had the best adsorption capacity.

Keywords: adsorption kinetics; coking coal; coking wastewater; modification

1. Introduction

Coking wastewater is mostly generated in the cooling step of coal coking at high temperature (900~1100 °C) and in the liquid-stripping step of the produced coke oven gas (COG) (Zhao et al., 2009). Moreover, massive quantities of condensed water are generated during the transportation of COG through pipelines to neighboring plants as a heat source (Kim et al., 2007). Coking wastewater contains complex inorganic and organic pollutants (Gao et al., 2016). These compounds are carcinogenic, mutagenic and toxic contaminants and may have long-term environmental and ecological impact. Therefore, the treatment of coking wastewater has been a significant research topic in wastewater treatment field.

Adsorption is widely used in wastewater treatment. However, the most widely and effectively used adsorbent is active carbon (Aksu and Yener 2001, Fan et al., 2016). Some studies indicate that active carbon achieves great effect on adsorbing dye, lignin, phenol, quinoline, pyridine, indole and other organic pollutants (Andersson et al., 2011, Ca, 2006, Carvajal-Bernal et al., 2015, Fletcher et al., 2007) . However, the usage of active carbon is limited by its difficult regeneration. Coal, as a natural polyporous materials possessing relative large surface area, stepped into researcher's sight. The result showed that the raw coal had great capacity and removal efficiency to adsorb heavy metal ions (Xia, 2000), organic pollutants (Cai and Tang, 2012, Cai et al., 2010), and copper in wastewater. The capacity of lignite to adsorb phenol was much larger than that generally observed with activated carbons when normalized for the surface areas (Polat et al., 2006). Some researchers also researched the effect of modified coal on

DOI: 10.5277/ppmp1898

its physicochemical properties. The results showed that the modified lignite (Wang et al., 2000), coal modified by organic solvent (CS_2), organic acid (CH_3COOH), inorganic acid (HCl) and strong oxidant (ClO_2) (Zhang et al., 2017), the modified brown coal (Wang et al., 2012)have well effect on wastewater treatment with structure change. So far, no studies have been reported on the treatment of coking wastewater by using modified coking coal., The advantage of coal adsorption method is that the adsorbent is cheap, disposable and widely available. The contaminated coal after adsorption will be returned to the coking plant, power plant or coal-water slurry plant without reducing the use value.

This research investigates the feasible modified methods of coking coal for removing organic pollutants such as quinoline, pyridine and phenol which are not easily biodegradable in coking wastewater and provides new modification method of coal utilization as adsorbent, which can improve the utilization value of coal., The adsorbents were characterized and the functional groups were measured. The adsorption behavior was investigated by adsorption kinetics.

2. Materials and methods

2.1 Materials

The coking coal used in this study was obtained from a coal preparation plant in Xuzhou, Jiangsu province, China. The coal samples belong to concentrate of gravity separation with particle size less than 25 mm, and then they were crushed and grounded to below 74 μm which were used as the absorbents. Surface modifications were carried out using solutions of 5 mol/dm^3 sodium hydroxide (NC), hydrochloric acid (HC), acetic acid (CC) as modifying agents; the ratio of coking coal to modifying agent was 1:4 w/w. The immersion was carried out at 25 °C and the samples were shaken up for 72 h with shaking speed of 120 rpm. After that, the samples were rinsed completely by deionized water. Finally, the samples were dried in an oven at 30 °C for 12 h. For the scenario of low-temperature oxidation surface modification, the samples were placed into the oven at 110 °C for 72 h.

Quinoline, pyridine and phenol with purity greater than 99.5% were purchased from Shanghai Chemical Company and used as a single component (adsorbate) in this study.

2.2 Characteristic analysis

The functional group analysis of adsorbents was measured by FT-IR instrument (VERTEX70v, Bruker Cor. Germany). The special surface area of adsorbents was measured by surface area analyzer (BELSORP-minill BET, MicrotracBEL Inc., Japan). Surface morphology of adsorbents were analyzed by the Scanning electron microscopy (SEM) (JSM-6700F, Japan).

Oxygen functional groups on the surface were characterized using the modified Boehm method (H.P et al., 1964). The method is adding 25 cm^3 of 0.05 mol/dm^3 NaOH to determine the acidic groups, and 25 cm^3 of 0.5 mol/dm^3 HCl solution to determine the basic groups in different flasks containing around 1.0000 g of each the modified coking coal., All samples were stirred at 25 °C for 24 h and then rinsed with deionized water until the rinse water kept a constant pH. Finally, the filtrate was titrated with 0.05 M NaOH or HCl.

2.3 Batch adsorption tests

The quinoline, pyridine and phenol solutions were prepared by dissolving the analytical reagent in deionized water. 2.0000 g adsorbent and 50 cm^3 adsorbate solution were added to the solutions in 100 cm^3 flasks mounted on a constant temperature (25 °C) water bath shaker at 120 rpm to keep the adsorbent suspended. All samples were filtered using needle tip filter with 0.045 μm pore size. The quinoline, pyridine, phenol concentrations of aqueous samples were measured by the UV/VIS spectrophotometer (Mei Puda 3500 UV/VIS, China). The removal of quinoline, pyridine and phenol from the aqueous samples was determined by UV adsorption and calculated using the formula:

$$q_t = \frac{(C_0 - C_t)V}{M} \quad (1)$$

where q_t (mg·g^{-1}) is the organic pollutants removed at time t by a unit mass of adsorbent, C_0 (mg/dm^3) is the initial organic pollutants concentration, C_t (mg/dm^3) is the organic pollutants concentration at time t, M (g/dm^3) is the amount of adsorbent added and V (dm^{-3}) is the adsorbate solutions volume.

To observe the effect of the adsorption time for absorbance and to collect kinetics data, parallel experiments were performed in various time from 10 to 180 min. The concentration of initial organic pollutants was 50 mg/dm^3, corresponding to the concentration in wastewater from the coal gas company. The residual concentration was measured by UV/VIS spectrophotometer.

2.4 Kinetics analysis

To investigate the process of quinoline, pyridine and phenol adsorption on coal, four kinetic models were employed to fit the data obtained.

2.4.1 Pseudo-first-order model

The pseudo-fist-order equation is given as:

$$\frac{\mathrm{d}q_t}{\mathrm{d}t} = K_1(q_{eq} - q_t) \tag{2}$$

where q_t is the amount of adsorbate adsorbed at time t (mg·g^{-1}), q_e the adsorption capacity at equilibrium (mg·g^{-1}), K_1 the pseudo-fist-order rate constant (min^{-1}) and t is the constant time (min). The integration of Eq. (2) with the initial condition, q_t=0 at t=0 leads to (Gerente et al., 2007):

$$\log(q_e - q_t) = \log q_e - \frac{\mathrm{K}_1}{2.303} t \ . \tag{3}$$

The values of adsorption rate constant (K_1) for quinoline, pyridine, phenol were determined from the plot of log (q_e - q_t) versus t.

2.4.2 Pseudo-second-order model

The pseudo-second-order model can be represented in the following form (Badmus and Audu 2009):

$$\frac{\mathrm{d}q_t}{\mathrm{d}t} = \mathrm{K}_2(q_e - q_t)^2 \tag{4}$$

where K_2 is the pseudo-second-order rate constant (g·mg^{-1}·min^{-1}). Integrating Eq. (4) and noting that q_t =0 at t=0, the following equation is obtained:

$$\frac{t}{q_t} = \frac{1}{\mathrm{K}_2 {q_e}^2} + \frac{t}{q_e} \tag{5}$$

The initial sorption rate h (mg·g^{-1}·min^{-1}), at $t \rightarrow 0$ is defined as:

$$h = \mathrm{K}_2 \times {q_e}^2 \ . \tag{6}$$

2.4.3 Intra-particle diffusion study

The possibility of intra-particle diffusion was explored by using the intra-particle diffusion model (Srivastava et al., 2005):

$$q_t = \mathrm{K}_3 t^{0.5} + \mathrm{I} \tag{7}$$

where K_3 is the intra-particle diffusion rate constant (mg·g^{-1}·min$^{-0.5}$) and I is the intercept (mg·g^{-1}). According to Eq. (7), a plot of q_t versus $t^{0.5}$ should be a straight line with a slope K_3 and intercept I when adsorption mechanism follows the intra-particle diffusion process.

3. Result and discussion

3.1 Characterization of adsorbents

The FTIR spectroscopy of several adsorbents are shown in Fig. 1. There is no significant change on the species of functional groups for all the adsorbents. A broad band between 3200 and 3600 cm^{-1} for all the adsorbents indicates the present of phenolic hydroxyl groups on the adsorbent surface (Sarkar et al., 2007). The IR spectra of all the adsorbents shows weak and broad peaks in the region of 2800-3000 cm^{-1} corresponding to CH_2 and CH_3 groups stretching from aliphatic or cycloalkane (Guo and Bustin 1998). The peak at 1600 cm^{-1} and weak peak in 2840 cm^{-1} corresponds to aldehydes and ketone groups (Ledesma et al., 1998). The FTIR spectra of the sample showed transmittance in the 1032 cm^{-1} region due to the ash, such as kaolin (Zhu 2001). The band 1386-1534 cm^{-1} may be attributed to the aromatic groups.

The peak at 550 cm^{-1} may be attributed to S-S in aromatics (Sarkar et al., 2007).

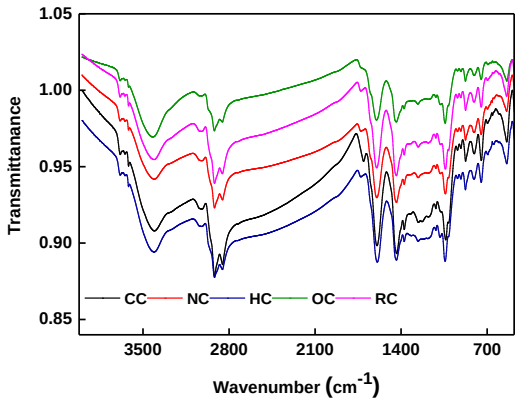

Fig. 1. FTIR spectroscopy of various adsorbents

SEM of the adsorbents is shown in Fig. 2. Compared with the original coking coal, the surfaces of coal modified by hydrochloric acid and acetic acid have more mounds, cracks, scraps and fragments, while the surface of samples modified by sodium hydroxide and low-temperature oxidation are relatively smooth.

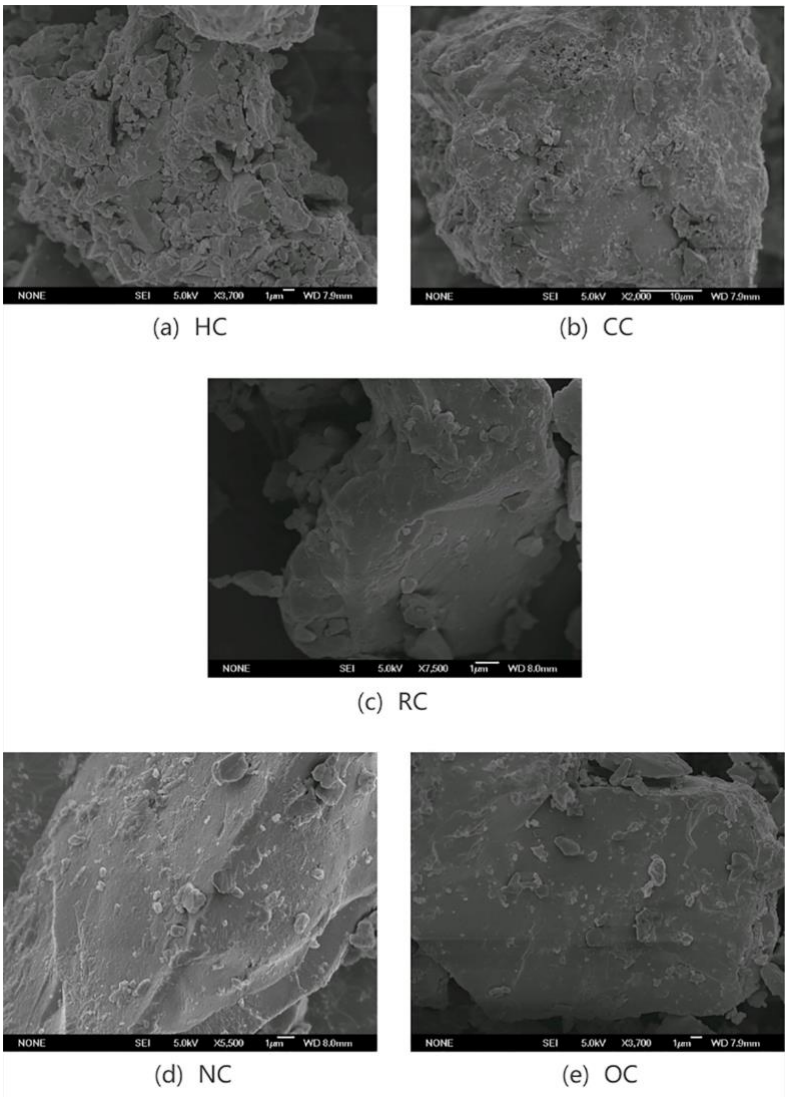

Fig. 2. Scanning electron micrograph of (a), (b), (c), (d), (e)

Table 1. Chemical parameters of different adsorbents

Sample	HC	CC	RC	NC	OC
Total acidity/μmol·g^{-1}	219.81	240.99	195.15	188.38	215.23
Total basicity/μmol·g^{-1}	186.35	192.00	208.25	220.35	218.58
Total groups/μmol·g^{-1}	406.16	432.99	403.40	408.73	433.81

The surface areas were calculated using the BET model (Kaya et al., 2013), and the surface areas were 10.336 m^2·g^{-1}, 10.722 m^2·g^{-1}, 11.625 m^2·g^{-1}, 13.629 m^2·g^{-1} and 14.592 m^2·g^{-1} for OC, NC, RC, HC and CC, respectively. The results correspond to the surface morphology of scanning electron micrograph. Compared with RC, the surface areas of CC and HC increased by 2.967 m^2·g^{-1}, 2.004 m^2·g^{-1}, respectively, while NC and OC decreased by 0.903 m^2·g^{-1}, 1.289 m^2·g^{-1}, respectively.

The total acidity and basicity of these five different absorbents are shown in Table 1. The values of acidity from high to low follow the order: CC, HC, OC, RC, NC. Compared with raw coal, the acidity value of HC, CC and OC have an increase, and the acidity of HC and OC are similar in values, while the sample of NC have a decrease. For the basicity, taken the RC for comparison the samples of NC and OC increase by 12.10 μmol·g^{-1} and 10.33 μmol·g^{-1}, respectively, while the samples of CC and HC decrease by 16.25 μmol·g^{-1} and 21.90 μmol·g^{-1}, respectively.

3.2 Effect of contact time on coal adsorption

The effect of contact time (t) on the removal of quinoline, pyridine, and phenol by different adsorbents are shown in Fig. 3. The contact time curves show that the adsorption capacity increased gradually before 60 min and reached quasi-equilibrium after 120 min, beyond which there was no significant increase in adsorption capacity. Fig. 3 (a) shows that the adsorption capacity of quinoline are increased by 0.19 mg·g^{-1}, 0.03 mg·g^{-1} respectively for CC and HC comparing with raw coking coal because of the maximum surface areas and functional groups; while the adsorption capacity of NC and OC are decreased by 0.09 mg·g^{-1}, 0.22 mg·g^{-1}, respectively. The most adsorption capacity and removal efficiency of quinoline are 1.05 mg·g^{-1} and 84.06% for CC. According to Fig. 3 (b), the adsorption capacity trend for all adsorbents are similar with quinoline, but the adsorption capacity increases for all absents. The maximum and minimum adsorption capacity of pyridine are 1.13 mg·g^{-1} and 0.77 mg·g^{-1} for CC and OC, respectively. The result of Fig. 3 (c) shows that the adsorption capacity of phenol from high to low follows the order: CC, HC, RC, NC, OC. Compared with Fig. 3 (a) and (b), the adsorption capacity decreases owing to phenol possessing weak acidic.

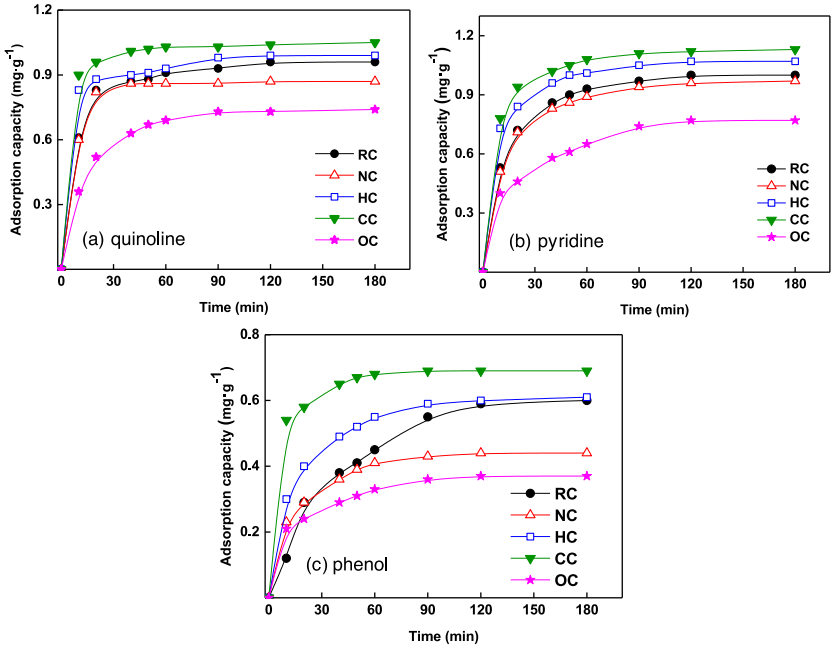

Fig. 3. Effect of contact time on the removal of quinoline, pyridine, phenol by various adsorbents

3.3 Adsorption kinetic models

3.3.1 Pseudo-first-order model

The data of adsorption experiments were analyzed by the function of origin 8.0 linear fitting, the results are shown in the Table 2. According to Table 2, the removal rate of quinoline indicated that he values for CC, RC, HC are similar and they are faster than NC, OC. The results owing to the adsorption rate is positively correlated with the specific surface area. The removal rate of pyridine from high to low follows the order: CC, HC, OC, RC, NC. The adsorption rate not only correlated with the specific surface area, but also correlated with the functional groups. The OC's removal rate of pyridine is faster than RC, because the OC possesses more functional groups. The value for the removal rate of phenol is bigger on CC followed by that on RC, NC, HC, OC in the order. The HC removal rate of phenol is slower than RC because the phenol is faintly acid and the acid functional groups are not conducive to the adsorption of phenol. For all the adsorbents to adsorb quinoline, pyridine and phenol, the adsorption process do not follow the pseudo-first-order model because the correlation coefficient is small and the $q_{e,\,meas}$ values are far bigger than the $q_{e,\,calc}$.

Table 2. Kinetics parameters of pseudo-first-order model for different absorptions

Adsorbate	Adsorbent	Pseudo-first-order model			
		$q_{e,meas}$/mg·g^{-1}	$q_{e,calc}$/mg·g^{-1}	K_1/min^{-1}	R^2
Quinoline	RC	0.96	0.59	0.0439	0.9362
	NC	0.87	0.13	0.0393	0.8630
	HC	0.99	0.42	0.0426	0.9148
	CC	1.05	0.13	0.0458	0.9135
	OC	0.74	0.50	0.0385	0.9376
Pyridine	RC	1.00	0.67	0.0381	0.9150
	NC	0.97	0.58	0.0371	0.9269
	HC	1.07	0.62	0.0426	0.9655
	CC	1.13	0.67	0.0481	0.9561
	OC	0.77	0.51	0.0419	0.9348
Phenol	RC	0.60	0.38	0.0364	0.9285
	NC	0.44	0.34	0.0362	0.9327
	HC	0.61	0.46	0.0352	0.9979
	CC	0.69	0.28	0.0488	0.9881
	OC	0.37	0.25	0.0304	0.9897

3.3.2 Pseudo-second-order model

Fig. 4 shows the plot of t/q_t versus t. The equilibrium adsorption capacity, $q_{e,calc}$ is obtained from the slope of the plot and the initial sorption rate h is obtained from the intercept. Since $q_{e,\,calc}$ is known from the slope, the pseudo-second-order constant K_2 can be determined from the value of the initial sorption rate. The $q_{e,\,meas}$ and the $q_{e,\,calc}$ values along with calculated non-linear correlation coefficients for pseudo-second-order models are shown in Table 3. The $q_{e,\,meas}$ (in Table 2) and the $q_{e,\,calc}$ values from the pseudo-second-order kinetic model are very close to each other. The correlation coefficients are also closer to unity for pseudo-second-order kinetics from 0.9855 to 0.9999. Therefore, the sorption can be approximated more appropriately by the pseudo-second-order kinetic model than the first-order kinetic model for all the adsorbents. The K_2 and h values as calculated from the Fig. 4 are listed in Table 3. The K_2 and h values for adsorption on CC is the highest due to the CC has the biggest surface areas and the relatively high functional groups.

Table 3. Kinetics parameters of pseudo-second-order model for different absorptions

Adsorbate	Adsorbent	Pseudo-second-order model			
		$q_{e,calc}$/mg·g^{-1}	K_2/g·mg^{-1}·min^{-1}	h/mg·g^{-1}·min^{-1}	R^2
Quinoline	RC	1.00	0.1697	0.1693	0.9993
	NC	0.88	0.3323	0.4145	0.9996
	HC	1.01	0.2429	0.2501	0.9995
	CC	1.06	0.4679	0.5266	0.9999
	OC	0.79	0.1316	0.0817	0.9993
Pyridine	RC	1.06	0.1018	0.1150	0.9998
	NC	1.01	0.1294	0.1332	0.9994
	HC	1.11	0.1565	0.1935	0.9999
	CC	1.16	0.1795	0.2417	0.9999
	OC	0.85	0.0739	0.0532	0.9969
Phenol	RC	0.75	0.0338	0.0191	0.9855
	NC	0.48	0.1827	0.0416	0.9994
	HC	0.65	0.1284	0.0544	0.9994
	CC	0.71	0.4467	0.2214	0.9999
	OC	0.40	0.1975	0.0388	0.9985

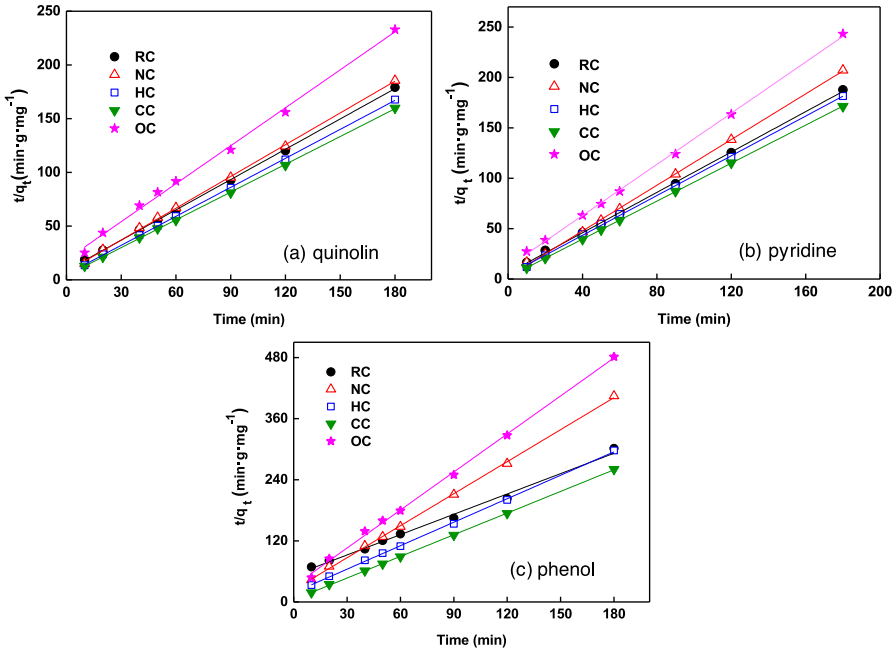

Fig. 4. Pseudo-second-order kinetic plots for the removal of quinoline, pyridine, phenol by various adsorbents

3.3.3 Intra-particle diffusion model

According to Eq. (7), a plot of q_t versus $t^{0.5}$ should be a straight line with a slope K_3 and intercept I when adsorption mechanism follows the intra-particle diffusion process. Fig. 5 presents a plot of q_t versus $t^{0.5}$ for all the adsorbents. The value of I gives an idea about the thickness of the boundary layer, i.e. the larger the intercept the greater is the boundary layer effect (Mohan and Karthikeyan 1997). The deviation of the straight lines from the origin may be due to the difference in the rate of mass transfer during the initial and final stages of adsorption. It also indicates that the pore diffusion is not the rate-controlling step (Wu and Yu 2006). The initial curved portion is attributed to the bulk diffusion and the linear portion to intra-particle diffusion (Andersson et al., 2011).

Table 4. Kinetics parameters of inter-particle diffusion model for different absorptions

Adsorbate	Adsorbent	Intra-particle diffusion		
		K_3/g ·mg^{-1} ·min$^{-0.5}$	I	R^2
Quinoline	RC	0.0332	0.6017	0.7167
	NC	0.0179	0.6849	0.4436
	HC	0.0172	0.7899	0.9220
	CC	0.0131	0.9029	0.7310
	OC	0.0336	0.3712	0.7467
Pyridine	RC	0.0425	0.5308	0.7772
	NC	0.0316	0.6045	0.8734
	HC	0.0320	0.7169	0.7994
	CC	0.0303	0.7914	0.7575
	OC	0.0400	0.3093	0.9054
Phenol	RC	0.0454	0.0691	0.8914
	NC	0.0208	0.2104	0.8252
	HC	0.0291	0.2780	0.8285
	CC	0.0172	0.1756	0.8805
	OC	0.0143	0.5357	0.7293

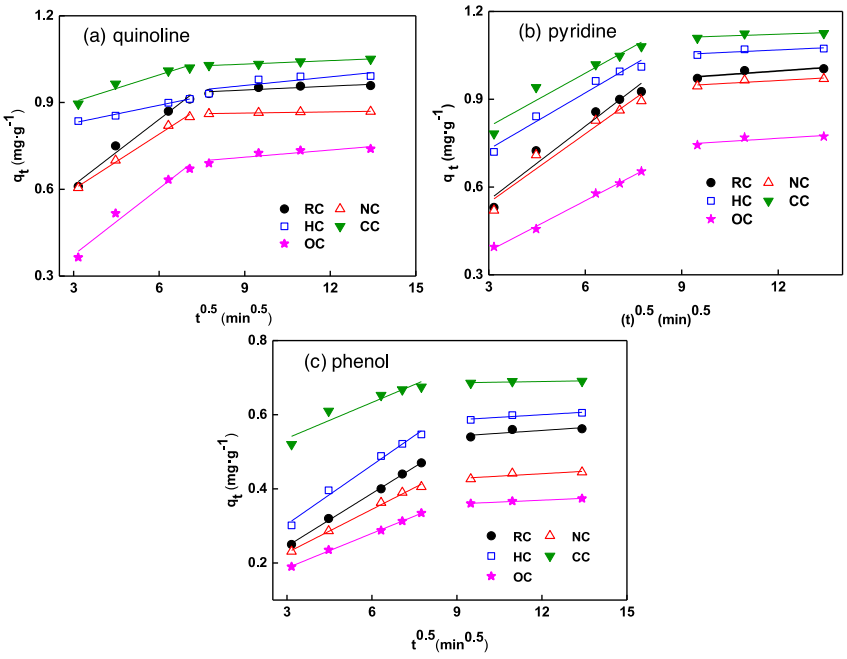

Fig. 5. Intra-particle diffusion plots for the removal of quinoline, pyridine, phenol by various adsorbents

4. Conclusions

The modification method with acetic acid has the highest adsorption capacity for the three organic pollutions. The adsorption capacity for CC of quinoline, pyridine, phenol is 1.05 mg ·g^{-1}, 1.13 mg ·g^{-1}, 0.69 mg ·g^{-1}, respectively. The surface area of CC and HC increased by 2.967 m^2 ·g^{-1} and 2.004 m^2 ·g^{-1} respectively compared with RC, which provides a new method to modify coal and coking coal modified with acid have bigger surface area. It is the significant aspect for adsorbents to adsorb quinoline, pyridine and phenol. Fitting of experimental data to various kinetics models showed that the processes fit well pseudo-second-order rate kinetics. To assess how the modifications effect adsorption process,

further investigations using column operations are recommended. This paper provides a new way to achieve the zero emissions of coking wastewater, which is very significance for wastewater purification.

Acknowledgements

This work was supported by the supported by National Natural Science Foundation of China (NO.51604280 and 51504262).

References

AKSU, Z. & J. YENER, 2001. *A comparative adsorption/biosorption study of mono-chlorinated phenols onto various sorbents*. Waste Manage (Oxford), 21, 695-702.

ANDERSSON, K. I., M. ERIKSSON & M. NORGREN, 2011. *Removal of Lignin from Wastewater Generated by Mechanical Pulping Using Activated Charcoal and Fly Ash: Adsorption Kinetics*. Ind Eng Chem Res, 50, 7733-7739.

BADMUS, M. A. O. & T. O. K. AUDU, 2009. *Periwinkle shell: Based granular activated carbon for treatment of chemical oxygen demand (COD) in industrial wastewater*. Can J Chem Eng, 87, 69–77.

CA, B., 2006. *Applicability of the various adsorption models of three dyes adsorption onto activated carbon prepared waste apricot*. J Hazard Mater, 135, 232-241.

CAI, C. F. & C. G. TANG, 2012. *Competitive adsorption of main organic pollutants from coking wastewater on coking coal.*, Journal of China Coal Society, 37, 1753-1759.

CAI, C. F., X. Q. ZHENG, G. HUI & M. J. ZUO, 2010. *Adsorption kinetics of organic in coking wastewater effluent from secondary sedimentation tank on coal.*, Journal of China Coal Society, 35, 299-302.

CARVAJAL-BERNAL, A. M., F. G MEZ, L. GIRALDO & J. C. MORENO-PIRAJ N, 2015. *Adsorption of phenol and 2,4-dinitrophenol on activated carbons with surface modifications*. Microporous & Mesoporous Materials, 209, 150-156.

FAN, G., J. LIU, Y. CAO, L. FENG & H. XU, 2016. *Adsorption mechanism of sodium oleate on titanium dioxide coated sensor surface using quartz crystal microbalance with dissipation*. Physicochemical Problems of Mineral Processing, 52, 597-608.

FLETCHER, A. J., A. YAPRAK UYGUR & K. M. THOMAS, 2007. *Role of Surface Functional Groups in the Adsorption Kinetics of Water Vapor on Microporous Activated Carbons*. Journal of Physical Chemistry C, 111, 8349-8359.

GAO, L., S. LI & Y. WANG, 2016. *Effect of different pH coking wastewater on adsorption of coking coal.*, Water Science & Technology 73, 582.

GERENTE, C., V. K. C. LEE, P. L. CLOIREC & G. MCKAY, 2007. *Application of Chitosan for the Removal of Metals From Wastewaters by Adsorption – Mechanisms and Models Review*. Critical Reviews in Environmental Science & Technology, 37, 41-127.

GUO, Y. & R. M. BUSTIN, 1998. *FTIR spectroscopy and reflectance of modern charcoals and fungal decayed woods: implications for studies of inertinite in coals*. International Journal of Coal Geology, 37, 29-53.

H.P, W. S. A. T., D. E, H. W & S. R, 1964. *Surface Oxides of Carbon*. Angew Chem Int Ed, 3, 669-677.

KAYA, E. M. Ö., A. S. ÖZCAN, Ö. G K & A. ÖZCAN, 2013. *Adsorption kinetics and isotherm parameters of naphthalene onto natural- and chemically modified bentonite from aqueous solutions*. Adsorption-journal of the International Adsorption Society, 19, 879-888.

KIM, Y. M., D. PARK, D. S. LEE & J. M. PARK, 2007. *Instability of biological nitrogen removal in a cokes wastewater treatment facility during summer*. J Hazard Mater, 141, 27-32.

LEDESMA, E. B., P. F. NELSON & J. C. MACKIE, 1998. *The formation of nitrogen species and oxygenated PAH during the combustion of coal volatiles*. Symposium on Combustion, 27, 1687-1693.

MOHAN, S. V. & J. KARTHIKEYAN, 1997. *Removal of lignin and tannin colour from aqueous solution by adsorption onto activated charcoal.*, Environ Pollut, 97, 183.

POLAT, H., M. MOLVA & M. POLAT, 2006. *Capacity and mechanism of phenol adsorption on lignite*. Int J Miner Process, 79, 264-273.

SARKAR, M., A. R. SARKAR & J. L. GOSWAMI, 2007. *Mathematical modeling for the evaluation of zinc removal efficiency on clay sorbent*. J Hazard Mater, 149, 666.

SRIVASTAVA, V. C., I. D. MALL & I. M. MISHRA, 2005. *Treatment of pulp and paper mill wastewaters with poly aluminium chloride and bagasse fly ash*. Colloids & Surfaces A Physicochemical & Engineering Aspects, 260, 17-28.

WANG, M. J., C. H. FU, L. P. CHANG & K. C. XIE, 2012. *Effect of fractional step acid treatment process on the structure and pyrolysis characteristics of Ximeng brown coal.*, Journal of Fuel Chemistry & Technology, 40, 906-911.

WANG, X. H., L. FENG, X. C. LIU, Y. ZHANG & M. ZHANG, 2000. *Effect of NaOH treatment on Water Sorption of*

Lignite. Research & Exploration in Laboratory, 33**,** 19-20.

WU, J. & H. Q. YU, 2006. *Biosorption of 2,4-dichlorophenol from aqueous solution by Phanerochaete chrysosporium biomass: isotherms, kinetics and thermodynamics*. J Hazard Mater, 137**,** 498-508.

XIA, C. B., HE, XIANGZHU, 2000. *Adsorption heavy metal ion for sulfonated lignite*. Material Protection, 33**,** 19-20.

ZHANG, X., Z. HAO, S. ZHANG & Y. YANG, 2017. *Difference of nano-scale pore changes and its control mechanism for tectonic coal under solvent reconstruction*. Journal of China University of Mining & Technology, 46**,** 148-154.

ZHAO, W. T., X. HUANG & D. J. LEE, 2009. *Enhanced treatment of coke plant wastewater using an anaerobic–anoxic–oxic membrane bioreactor system*. Separation & Purification Technology, 66**,** 279-286.

ZHU, H., LI, HU LIN , OU, ZHESHEN , WANG, DIANZUO, XIAOLI LV, 2001. *Study on Surface Modification of Different Rank Coals by Using FTIR*. Journal of China University of Mining &Technology, 30**,** 366-370.